JOURNAL OF NATURAL PRODUCTS

pubs.acs.org/jnp

Article

Motobamide, an Antitrypanosomal Cyclic Peptide from a *Leptolyngbya* sp. Marine Cyanobacterium

Hiroki Takahashi, Arihiro Iwasaki, Naoaki Kurisawa, Ryota Suzuki, Ghulam Jeelani, Teruhiko Matsubara, Toshinori Sato, Tomoyoshi Nozaki, and Kiyotake Suenaga*

Cite This: *J. Nat. Prod.* 2021, 84, 1649−1655

Read Online

ACCESS | Metrics & More | Article Recommendations | Supporting Information

ABSTRACT: Motobamide (**1**), a new cyclic peptide containing a *C*-prenylated cyclotryptophan residue, was isolated from a marine *Leptolyngbya* sp. cyanobacterium. Its planar structure was established by spectroscopic and MS/MS analyses. The absolute configuration was elucidated based on a combination of chemical degradations, chiral-phase HPLC analyses, spectroscopic analyses, and computational chemistry. Motobamide (**1**) moderately inhibited the growth of bloodstream forms of *Trypanosoma brucei rhodesiense* (IC_{50} 2.3 μM). However, it exhibited a weaker cytotoxicity against normal human cells (IC_{50} 55 μM).

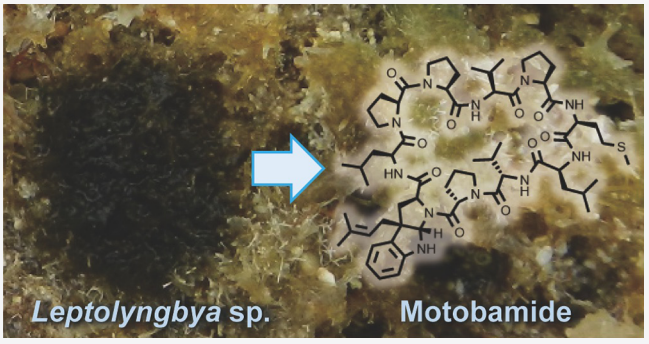

African sleeping sickness, one of the neglected tropical diseases, is caused by the protozoa *Trypanosoma brucei rhodesiense* and *Trypanosoma brucei gambiense* and threatens human health, mainly in sub-Saharan Africa.[1] As African sleeping sickness is a fatal disease without any therapy, effective antitrypanosomal drugs are essential for people living in areas where this disease is endemic. However, existing antitrypanosomal drugs have several problems, such as serious side effects and emergence of drug-resistant strains.[1] Therefore, the discovery of new lead compounds is desired for the development of more effective drugs.

Marine cyanobacteria have gained attention as rich sources of bioactive secondary metabolites. In fact, several antiparasitic natural products, such as almiramides B and C, which exhibit antileishmanial activity,[2] and ikoamide, which shows antimalarial activity,[3] have been isolated from marine cyanobacteria. Hence, we investigated the secondary metabolites of marine cyanobacteria as a source for antitrypanosomal drugs. As a result, we isolated a new antitrypanosomal compound, motobamide (**1**), from a *Leptolyngbya* sp. marine cyanobacterium. Structurally, **1** is a cyclic decapeptide that contains an unusual *C*-prenylated cyclotryptophan residue. Motobamide (**1**) showed stronger antitrypanosomal activity than cytotoxicity against normal human cells, WI-38. Here we report the isolation, structure determination, and biological activities of motobamide (**1**).

RESULTS AND DISCUSSION

A *Leptolyngbya* sp. marine cyanobacterium (1.1 kg, wet weight) was collected at Bisezaki, Okinawa, Japan, in April 2018. The sample was extracted with EtOH, and the extract was filtered, concentrated, and partitioned between EtOAc and H_2O. The EtOAc-soluble material was further partitioned between 90% aqueous MeOH and hexane. The aqueous MeOH fraction was subjected to fractionation by reversed-phase column chromatography (ODS silica gel, MeOH−H_2O) and repeated reversed-phase HPLC to give motobamide (**1**, 0.6 mg).

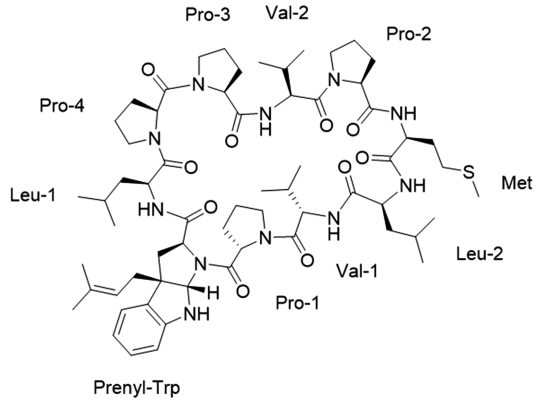

Motobamide (**1**)

Received: March 12, 2021
Published: May 13, 2021

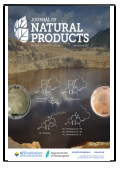

Table 1. NMR Data for Motobamide (1) in CD_3OD

unit	position	δ_C,[a] type	δ_H[b] (J in Hz)	COSY correlations	selected HMBC correlations	selected NOESY correlations
Leu-1	1	173.2,[c] C				
	2	50.6, CH	4.76, dd (9.2, 5.5)	3	1	63a, 63b
	3	41.7, CH_2	1.58, m	2, 4		
	4	25.1, CH	1.73, m	3, 5, 6		
	5	24.2, CH_3	0.98, d (7.2)	4		
	6	21.5, CH_3	0.96, d (6.7)	4		
Prenyl-Trp	7	175.6, C				
	8	63.1, CH	4.13, m	9a, 9b	7	25a, 25b
	9a	42.7, CH_2	2.79, dd (13.3, 8.2)	8, 9b	10, 16	
	9b		2.36, m	8, 9a	10	
	10	56.9, C				
	11a	35.1, CH_2	2.42, m	11b, 12	10	
	11b		2.34, m	11a, 12	10	
	12	120.1, CH	5.19, t (6.9)	11a, 11b, 14, 15	14, 15	14, 16
	13	136.9, C				
	14	26.2,[d] CH_3	1.72, s	12	13	12
	15	18.2, CH_3	1.57, s	12	12, 13	
	16	84.8, CH	5.53, s		8, 11, 17, 22	12
	17	133.3, C				
	18	124.1, CH	7.13, d (7.8)	19, 20, 21	10	
	19	120.2, CH	6.74, t (7.8)	18, 20, 21	17	
	20	129.6, CH	7.05, t (7.8)	18, 19, 21	22	
	21	110.5, CH	6.64, d (7.8)	18, 19, 20		
	22	149.6, C				
Pro-1	23	173.5,[e] C				
	24	61.2, CH	4.15, m	25		
	25a	29.13, CH_2	2.06, m	24, 25b, 26a, 26b	23	8
	25b		1.35, m	24, 25a, 26a, 26b	23	8
	26a	25.6,[f] CH_2	2.09, m	25a, 25b, 26b, 27		
	26b		1.96, m	25a, 25b, 26a, 27		
	27	49.1, CH_2	3.73, t (6.9)	26a, 26b		29
Val-1	28	172.9,[c] C				
	29	57.4, CH	4.63, d (7.4)	30	28, 33	27
	30	33.5, CH	2.16, m	29, 31, 32		
	31	20.0, CH_3	1.13, d (6.9)	30		
	32	18.5, CH_3	1.06, d (6.9)	30		
Leu-2	33	175.0, C				
	34	56.6, CH	4,16, m	35a, 35b	33	
	35a	41.2, CH_2	2.00, m	34, 35b, 36		
	35b		1.59, m	34, 35a, 36		
	36	26.1,[d] CH	1.79, m	35a, 35b, 37, 38		
	37	23.9, CH_3	1.04, d (6.4)	36		
	38	21.3, CH_3	0.96, d (6.7)	36		
Met	39	174.2,[e] C				
	40	53.2, CH	3.78, dd (11.0, 3.1)	41a, 41b	39	46a, 46b
	41a	not detected	2.20, m	40, 41b, 42		
	41b		2.04, m	40, 41a, 42		
	42	31.0, CH_2	2.44, m	41a, 41b		
	43	14.8, CH_3	1.93, s		42	
Pro-2	44	173.0,[c] C				
	45	61.7, CH	4.44, m	46		
	46a	30.0, CH_2	1.87, m	45, 46b, 47a, 47b	44	40
	46b		1.58, m	45, 46a, 47a, 47b		40
	47a	26.1, CH_2	2.05, m	46a, 46b, 47b, 48a, 48b		
	47b		1.68, m	46a, 46b, 47a, 48a, 48b		
	48a	49.0, CH_2	3.63, m	47a, 47b, 48b		50
	48b		3.50, m	47a, 47b, 48a		50
Val-2	49	170.7, C				
	50	58.1, CH	4.53, d (10.5)	51	49	48a, 48b
	51	31.4, CH	2.22, m	50, 52, 53		
	52	20.0, CH_3	0.912, d (6.9)	51		

https://doi.org/10.1021/acs.jnatprod.1c00234
J. Nat. Prod. 2021, 84, 1649−1655

Table 1. continued

unit	position	δ_C,[a] type	δ_H[b] (J in Hz)	COSY correlations	selected HMBC correlations	selected NOESY correlations
	53	18.8, CH_3	0.907, d (6.9)	51		
Pro-3	54	173.4,[e] C				
	55	62.4, CH	4.47, m	56a, 56b	54	60
	56a	33.1, CH_2	2.33, m	55, 56b, 57a, 57b		
	56b		2.23, m	55, 56a, 57a, 57b		
	57a	23.2, CH_2	1.96, m	56a, 56b, 57b, 58a, 58b		
	57b		1.80, m	56a, 56b, 57a, 58a, 58b		
	58a	48.3, CH_2	3.68, m	57a, 57b, 58b		
	58b		3.49, m	57a, 57b, 58a		
Pro-4	59	173.1,[e] C				
	60	60.1, CH	4.23, dd (8.8, 4.6)	61a, 61b		55
	61a	29.13, CH_2	2.30, m	60, 61b, 62a, 62b		
	61b		1.87, m	60, 61a, 62a, 62b		
	62a	25.7;[f] CH_2	2.06, m	61a, 61b, 62b, 63a, 63b		
	62b		2.02, m	61a, 61b, 62a, 63a, 63b		
	63a	48.2, CH_2	3.91, m	62a, 62b, 63b		2
	63b		3.64, m	62a, 62b, 63a		2

[a]Measured at 100 MHz. [b]Measured at 400 MHz. [c−f]These carbon signals are interchangeable.

Motobamide (**1**) was obtained as a colorless oil. The molecular formula of **1** was found to be $C_{63}H_{95}N_{11}O_{10}S$ by HRESIMS (m/z 1220.6864). In the ^{1}H NMR spectrum (Table 1), one triplet signal at 5.19 ppm and two singlet methyl signals at 1.72 and 1.57 ppm indicated the presence of one carbon−carbon double bond and two vinyl methyl groups. In the ^{13}C NMR spectrum (Table 1), 10 signals (δ_C 175.6, 175.0, 174.2, 173.5, 173.4, 173.2, 173.1, 173.0, 172.9, and 170.7), considered to be amide or ester carbonyl carbons, were detected. In addition, detailed analyses of the 2D NMR spectra revealed the presence of nine proteogenic amino acids: two leucines (Leu), four prolines (Pro), two valines (Val), and a methionine (Met). Although we could not detect the carbon signal of C-41, the presence of a methylene group at C-41 was verified based on the COSY correlations (H-40/H-41a, H-40/H-41b, H-41a/H-42, and H-41b/H-42). In addition, we also clarified the presence of an unusual amino acid, *C*-prenylated cyclotryptophan (Prenyl-Trp), as follows. The COSY correlations (H-8/H-9a, H-8/H-9b, H-18/H-19, H-19/H-20, and H-20/H-21) revealed two partial structures (C-8−C-9 and C-18−C-19−C-20−C-21). In addition, two COSY correlations (H-11a/H-12 and H-11b/H-12), five HMBC correlations (H-12/C-14, H-12/C-15, H-14/C-13, H-15/C-12, and H-15/C-13), and their chemical shifts established the presence of a prenyl group. These three partial structures and four carbons (C-10, C-16, C-17, and C-22) were connected based on the HMBC correlations (H-9a/C-10, H-9b/C-10, H-9a/C-16, H-11a/C-10, H-11b/C-10, H-16/C-8, H-16/C-11, H-16/C-17, H-16/C-22, H-18/C-10, H-19/C-17, and H-20/C-22). Finally, we clarified the location of the two nitrogen atoms based on the deshielded chemical shifts of C-8 (δ_C 63.1, δ_H 4.13), C-16 (δ_C 84.8, δ_H 5.53), and C-22 (δ_C 149.6). As a result, these moieties formed a cyclic tryptophan residue with a prenyl side chain.

Next, we determined the sequence of these 10 amino acid residues (Figure 1). The HMBC correlation (H-29/C-33) and NOESY correlations (H-27/H-29, H-8/H-25a, and H-8/H-25b) revealed the following sequence: Prenyl-Trp-Pro-1-Val-1-Leu-2. Based on the NOESY correlations (H-40/H-46a, H-40/H-46b, H-48a/H-50, and H-48b/H-50), the segment of Met-Pro-2-Val-2 was established. Furthermore, the NOESY

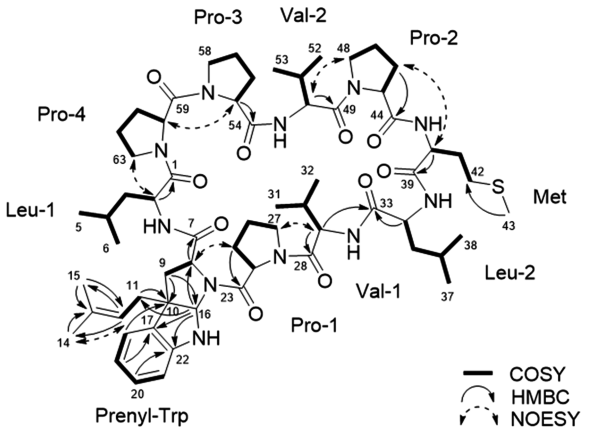

Figure 1. Gross structure of motobamide (**1**) based on 2D NMR analyses.

correlations (H-2/H-63a, H-2/H-63b, and H-55/H-60) established the sequence: Pro-3-Pro-4-Leu-1. As we could not get any additional structural information from NMR data, we carried out an MS/MS analysis of **1** to connect these three partial sequences (Figure 2). The MS/MS analysis showed three fragmentation patterns as shown in Figure 2, suggesting structure **1** for motobamide (**1**).

The geometries of the peptide bonds of the proline residues were determined based on the ^{13}C NMR chemical shift differences between the β and γ positions ($\Delta\delta_{\beta-\gamma}$).[4] The large difference observed in Pro-3 ($\Delta\delta_{\beta-\gamma}$ = 9.9 ppm) indicated that its peptide bond has a *cis* geometry. This conclusion was also supported by the NOESY correlation, H-55/H-60. On the contrary, the difference at Pro-1 ($\Delta\delta_{\beta-\gamma}$ = 3.5 ppm), Pro-2 ($\Delta\delta_{\beta-\gamma}$ = 3.9 ppm), and Pro-4 ($\Delta\delta_{\beta-\gamma}$ = 3.4 ppm) indicated that they possess a *trans* geometry, supported by the NOESY correlations (H-27/H-29, H-48a/H-50, H-48b/H-50, H-2/H-63a, and H-2/H-63b). The geometry of the peptide bond at the *C*-prenylated cyclotryptophan residue was determined to be *cis* on the basis of the NOESY correlations (H-8/H-25a and H-8/H-25b).

The absolute configurations of all the usual amino acids in motobamide (**1**) were determined by acid hydrolysis followed

https://doi.org/10.1021/acs.jnatprod.1c00234
J. Nat. Prod. 2021, 84, 1649−1655

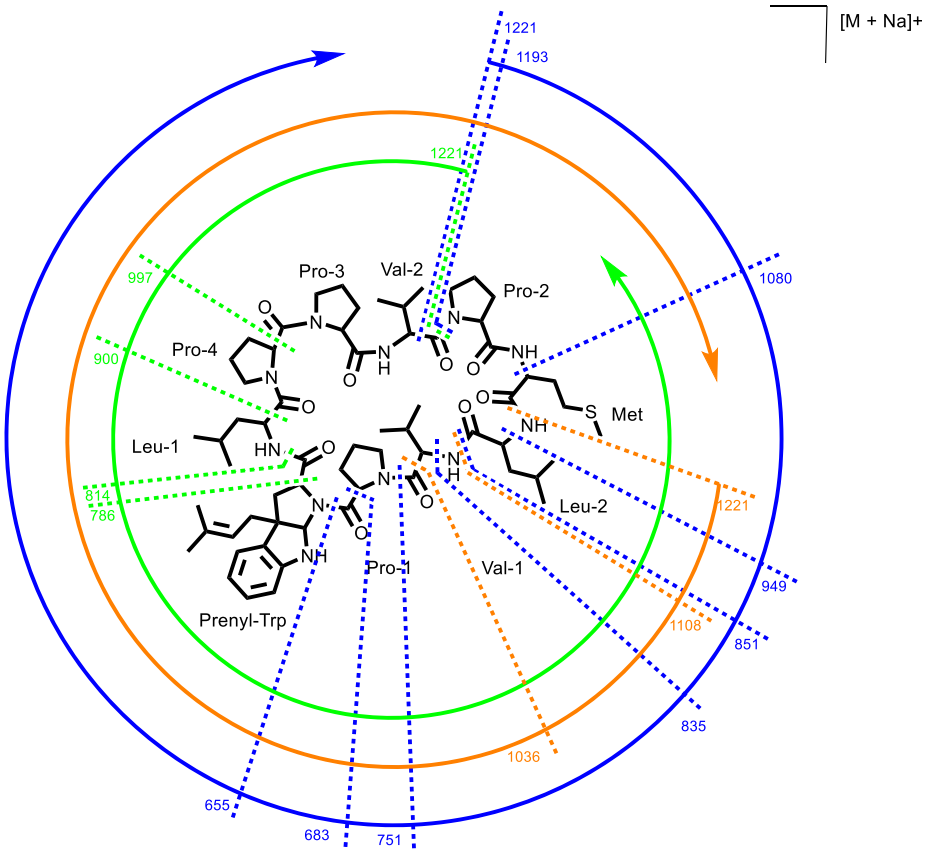

Figure 2. MS/MS fragmentation of motobamide (**1**).

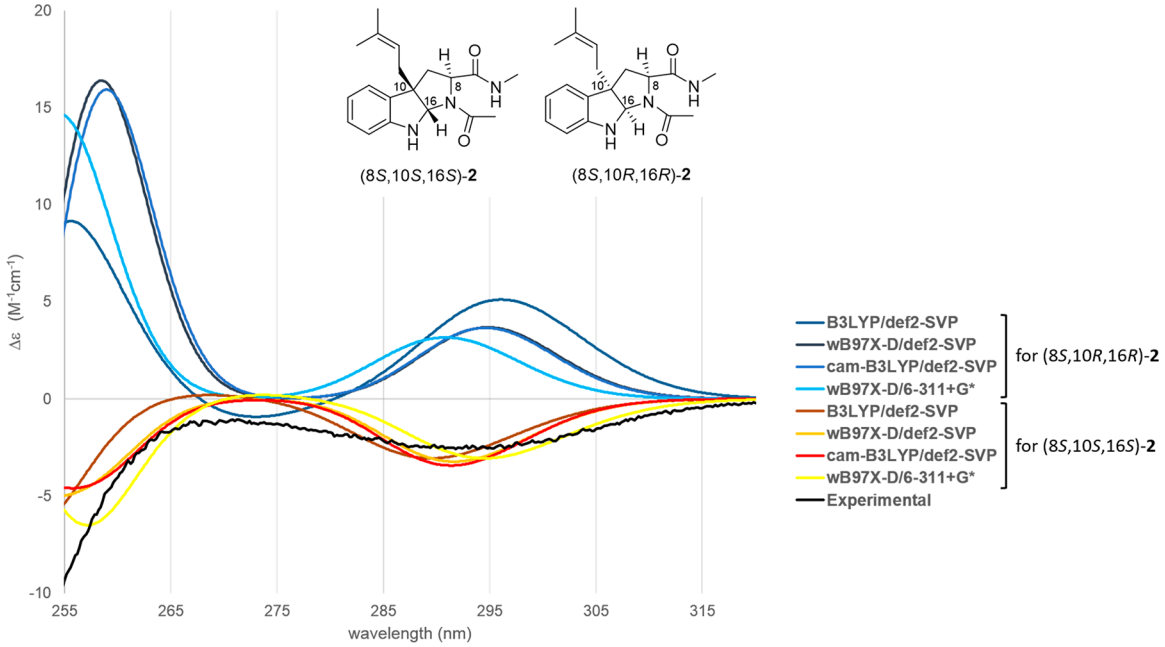

Figure 3. Experimental ECD spectrum of motobamide (**1**) and theoretical ECD spectra of the model compounds (8*S*,10*S*,16*S*)-**2** and (8*S*,10*R*,16*R*)-**2**.

by chiral-phase HPLC analyses. To make the results clear, we isolated each amino acid from the hydrolysate before chiral-phase HPLC analyses. These analyses revealed that they are all of the L form. As for Prenyl-Trp, acid hydrolysis of **1** with phenol afforded tryptophan derived from the Prenyl-Trp residue. Acid hydrolysis in the presence of phenol[5] and chiral-HPLC analysis afforded L-Trp (from Prenyl-Trp) and determined the absolute configuration of C-8 as *S*.

The NOESY correlation between H-12 and H-16 indicated that the prenyl group and H-16 are located on the same face of Prenyl-Trp. Therefore, there were two possible absolute configurations of Prenyl-Trp: (8*S*,10*S*,16*S*) and

https://doi.org/10.1021/acs.jnatprod.1c00234
J. Nat. Prod. 2021, 84, 1649−1655

(8*S*,10*R*,16*R*). The electronic circular dichroism (ECD) spectrum of motobamide (**1**) showed a negative Cotton effect at 295 nm, as shown in Figure 3. Considering the UV absorption wavelength of the functional groups in **1**, this Cotton effect was derived from the aromatic ring in the Prenyl-Trp residue. As the whole structure of **1** involves a large number of conformers to be considered, we designed the two simplified model compounds (8*S*,10*S*,16*S*)-**2** and (8*S*,10*R*,16*R*)-**2**. Next, we calculated theoretical ECD spectra of the model compounds using several pairs of basis function and functional, respectively, and compared them with that of natural **1** (Figure 3). The theoretical spectra of (8*S*,10*S*,16*S*)-**2** in all calculation conditions showed Cotton curves similar to that of **1**, suggesting the absolute configuration of the Prenyl-Trp residue as 8*S*, 10*S*, 16*S*.

Next, we evaluated the biological activity of motobamide (**1**). Motobamide (**1**) inhibited the growth of the bloodstream form of *T. b. rhodesiense*, the causative organism of human African sleeping sickness, with an IC_{50} value of 2.3 μM, while the cytotoxicity of **1** against WI-38 cells, normal human fibroblasts (IC_{50} = 55 μM), was more than 20-fold weaker. In addition, **1** did not show any growth-inhibitory activity against HeLa or HL60 cells at 10 μM.

In conclusion, we discovered a new modified cyclic decapeptide, motobamide (**1**), from a *Leptolyngbya* sp. marine cyanobacterium collected in Okinawa, Japan. The planar structure of **1** was established based on the analyses of 2D NMR and MS/MS spectra. The absolute configurations of the usual amino acids were established by acid hydrolysis followed by chiral-phase HPLC analyses. The absolute configuration of the unusual amino acid Prenyl-Trp was determined by a combination of experimental and computational calculation chemistry. Since some cyanobacteria produce Prenyl-Trp-containing compounds, i.e., kawaguchipeptin A[5] and trikoramide A,[6] the calculated ECD spectra of the two model compounds (8*S*,10*S*,16*S*)-**2** and (8*S*,10*R*,16*R*)-**2** can be useful for determining the absolute configuration of Prenyl-Trp units of these compounds. Motobamide (**1**) moderately inhibited the growth of bloodstream forms of *T. b. rhodesiense*, but did not show any cytotoxicity against human cells at 10 μM. Further evaluations of the antiparasitic potency of **1** are ongoing in our laboratory.

EXPERIMENTAL SECTION

General Experimental Procedures. Optical rotations were measured with a JASCO DIP-1000 polarimeter. UV spectra were recorded on a JASCO V730-BIO instrument. ECD spectra were measured with a JASCO J-720 W spectropolarimeter. IR spectra were recorded on a Bruker ALPHA instrument. All NMR data were recorded on a JEOL JNM-ECS400 spectrometer for ^{1}H (400 MHz) and ^{13}C (100 MHz). ^{1}H NMR chemical shifts (referenced to residual CD_3OD observed at δ_H 3.31) were assigned using a combination of data from COSY and HMQC experiments. Similarly, ^{13}C NMR chemical shifts (referenced to CD_3OD observed at δ_C 49.0) were assigned based on HMBC and HMQC experiments. HRESIMS spectra were obtained on a Waters LCT Premier XE time-of-flight (TOF) mass spectrometer. MS and MS^n spectra were collected in positive mode by using a Bruker Daltonics amaZon SL ion trap mass spectrometer equipped with an ESI source. Chromatographic analyses were performed using an HPLC system consisting of a pump (model PU-2080, JASCO) and a UV detector (model UV-2075, JASCO). All chemicals and solvents used in this study were the best grade available and obtained from a commercial source. Density functional theory (DFT) and time-dependent density functional theory (TDDFT) calculations were run with Gaussian 16 with default grids and convergence criteria.

Identification of the Cyanobacterium. A cyanobacterial filament was isolated under the microscope and crushed by freezing and thawing. The 16S rDNA genes were PCR-amplified from the isolated DNA using the primer set CYA359F (a cyanobacterial-specific primer) and CYA1371R (a universal primer). The PCR reaction contained DNA derived from the cyanobacteria filament, 0.5 μL of KOD-Multi & Epi- (Toyobo), 0.8 μL of each primer (0.4 μM, respectively), 12.5 μL of 2× PCR buffer for KOD-Multi & Epi-, and H_2O for a total volume of 25 μL. The PCR reaction was performed as follows: initial denaturation for 2 min at 94 °C and amplification by 40 cycles of 10 s at 98 °C and 1.5 min at 66 °C. PCR products were analyzed on agarose gel (1%) in TBE buffer and visualized by ethidium bromide staining. The obtained DNA was sequenced with CYA359F and CYA1371R primers. This sequence is available in the DDBJ/EMBL/GenBank databases under accession number LC602971. The nucleotide sequence of 16S rRNA gene obtained in this study was used for phylogenetic analysis with the sequences of related cyanobacterial 16S rRNA genes.[7] All sequences were aligned by the SINA web service (version 1.2.11)[8] with default settings. The poorly aligned positions and divergent regions were removed by Gblocks Server (version 0.91b),[9] implementing the options for a less stringent selection, including the 'Allow smaller final blocks', 'Allow gap positions within the final blocks', and 'Allow less strict flanking positions' options. The obtained 802 nucleotide positions were used for phylogenetic analysis. JModeltest (version 2.1.7)[10,11] with default settings was used to select the best model of DNA substitution for the Maximum Likelihood (ML) analysis and Bayesian analysis according to the Akaike information criterion (AIC). The ML analysis was conducted by PhyML (version 20131016),[11] using the TIM2+I+G model with a gamma shape parameter of 0.4280, a proportion of invariant sites of 0.4750, and nucleotide frequencies of F(A) = 0.2566, F(C) = 0.2155, F(G) = 0.3054, and F(T) = 0.2225. Bootstrap resampling was performed on 1000 replicates. The ML tree was visualized with Njplot (version 2.3).[12] The Bayesian analysis was conducted by MrBayes (version 3.2.5)[13] using the GTR+I+G model. The Markov chain Monte Carlo process was set at 2 chains, and 1 000 000 generations were conducted. Sampling frequency was assigned at every 500 generations. After analysis, the first 100 000 trees were deleted as burn-in, and the consensus tree was constructed. The Bayesian tree was visualized with FigTree (version 1.4.0, http://tree.bio.ed.ac.uk/software/figtree). As a result, the cyanobacterium (accession no. LC602971) formed a clade with *Leptolyngbya* sp. Therefore, the cyanobacterium was classified into *Leptolyngbya* sp.

Collection, Extraction, and Isolation. The *Leptolyngbya* sp. cyanobacterium (cell mass 1.1 kg, wet weight) was collected at Bise, Okinawa Island, Okinawa Prefecture, Japan, during April 2018. The collected cyanobacterium was extracted with EtOH (2 × 2 L) for 5 days. The extract was filtered, and the filtrate was concentrated. The residue was partitioned between EtOAc (3 × 0.3 L) and H_2O (0.3 L). The material obtained from the organic layer was partitioned between 90% aqueous MeOH (0.3 L) and hexane (3 × 0.3 L) to give an aqueous MeOH fraction (593 mg). The aqueous MeOH fraction was separated by column chromatography on ODS (6.0 g) eluted with 40% MeOH, 60% MeOH, 80% MeOH, MeOH, and $CHCl_3$−MeOH (1:1). The fraction eluted with 80% MeOH (143 mg) was subjected to HPLC [Cosmosil 5C_{18}MS-II (ϕ 20 × 250 mm); flow rate 5 mL/min; detection, UV 215 nm; solvent 80% aqueous MeOH] in five batches to give a fraction that contained motobamide (**1**) (58.8 mg, the last collected fraction). This fraction was further purified by HPLC [Cosmosil 5C_{18}MS-II (ϕ 20 × 250 mm); flow rate 5 mL/min; detection, UV 215 nm; solvent 85% aqueous MeOH] in two batches to give a motobamide (**1**)-containing fraction (8.9 mg, t_R = 44.8 min). Moreover, this fraction was subjected to HPLC [Cosmosil Cholester (ϕ 20 × 250 mm); flow rate 5 mL/min; detection, UV 215 nm; solvent aqueous 70% MeCN] to give a fraction that contained **1** (2.0 mg, t_R = 32.0 min). Finally, this fraction was purified by HPLC [Cosmosil 5PE-MS (ϕ 20 × 250 mm); flow rate 5 mL/min;

https://doi.org/10.1021/acs.jnatprod.1c00234
J. Nat. Prod. 2021, 84, 1649−1655

detection, UV 215 nm; solvent aqueous 63% MeCN] to give motobamide (**1**, 0.6 mg, t_R = 35.3 min).

Motobamide (1): colorless oil; $[\alpha]^{25}_D$ −243 (*c* 0.17, MeOH); UV (MeOH) λ_{max} (log ε) 238 (4.05), 295 (3.56) nm; ECD (0.83 mM, MeCN) λ_{max} ($\Delta\varepsilon$) 295 (−2.52) nm; IR (neat) 3307, 2960, 1641, 1527, 1446, 1310 cm^{-1}; ^1H NMR, ^{13}C NMR, COSY, HMBC, NOESY, and TOCSY data, Table 1; HRESIMS *m*/*z* 1220.6864 [M + Na]$^+$ (calcd for $C_{63}H_{95}N_{11}O_{10}SNa$, 1220.6882).

Determination of the Absolute Configuration of Motobamide (1). Motobamide (**1**, 0.2 mg) was treated with 6 M HCl (100 μL) for 18 h at 110 °C. The reaction mixture was evaporated to dryness and separated on an analytical HPLC column [conditions for HPLC separation: column, Cosmosil 5C_{18}-PAQ (ϕ 4.6 × 250 mm); flow rate, 1.0 mL/min; detection at 215 nm; solvent H_2O; retention times (min) of components: Pro (3.5), Val (3.7), Met (4.7), and Leu (5.4)].

Each fraction was dissolved in H_2O (50 μL) and analyzed by chiral-phase HPLC, and the retention times were compared to those of authentic standards [column, DAICEL CHIRALPAK MA (+) (ϕ 4.6 × 50 mm); flow rate, 1.0 mL/min; detection at 254 nm; solvent 2 mM $CuSO_4$]. The retention times for authentic standards were 2.9 min (D-Pro), 5.8 min (L-Pro), 3.8 min (D-Val), 6.7 min (L-Val), 6.8 min (D-Met), 11.2 min (L-Met), 8.1 min (D-Leu), and 15.3 min (L-Leu). The retention times of each amino acid from natural **1** were 5.8, 6.7, 11.2, and 15.3 min, indicating the presence of L-Pro, L-Val, L-Met, and L-Leu, respectively.

Motobamide (**1**, 0.1 mg) was treated with 1% phenol in 6 M HCl (100 μL) for 4 h at 110 °C.[5] The hydrolyzed product was evaporated to dryness, and Trp was isolated as a derivative of the Prenyl-Trp residue of **1** by HPLC separation [conditions for HPLC separation: column, Cosmosil 5C_{18}-PAQ (ϕ 4.6 × 250 mm); flow rate, 1.0 mL/min; detection at 215 nm; solvent 20% MeOH; retention time of Trp is 9.2 min]. The fraction was dissolved in H_2O (50 μL) and analyzed by chiral-phase HPLC, and the retention time was compared to those of authentic standards [column, DAICEL CHIRALPAK MA(+) (ϕ 4.6 × 50 mm); flow rate, 1.0 mL/min; detection at 254 nm; solvent 15% MeCN 2 mM $CuSO_4$]. The retention times for authentic standards were 8.8 min (D-Trp) and 10.8 min (L-Trp). The retention time of Trp from Prenyl-Trp of natural **1** was 10.8 min, indicating the presence of Prenyl-L-Trp.

Cell Growth Analysis. WI-38 cells and HeLa cells were cultured at 37 °C with 5% CO_2 in DMEM (Nissui) supplemented with 10% heat-inactivated fetal bovine serum (FBS), 100 units/mL penicillin, 100 μg/mL streptomycin, 0.25 μg/mL amphotericin, 300 μg/mL L-glutamine, and 2.25 mg/mL $NaHCO_3$. HL60 cells were cultured at 37 °C with 5% CO_2 in RPMI (Nissui) supplemented with 10% heat-inactivated FBS, 100 units/mL penicillin, 100 μg/mL streptomycin, 0.25 μg/mL amphotericin, 300 μg/mL L-glutamine, and 2.25 mg/mL $NaHCO_3$. WI-38 cells were seeded at 4 × 10^3 cells/well in 96-well plates (Iwaki) and cultured overnight. HeLa cells were seeded at 2 × 10^4 cells/well in 96-well plates (Iwaki) and cultured overnight. HL60 cells were seeded at 10 × 10^4 cells/well in 96-well plates. Various concentrations of compounds were then added, and cells were incubated for 72 h. Cell proliferation was measured by the MTT assay.

***In Vitro* Antitrypansomal Assay.** The bloodstream form of *Trypanosoma brucei rhodesiense* strains IL-1501[14] was cultured at 37 °C under a humidified 5% CO_2 atmosphere in HMI-9 medium[15] supplemented with 10% heat-inactivated FBS. For *in vitro* studies, compounds were dissolved in DMSO and diluted in culture medium prior to being assayed. The maximum DMSO concentration in the *in vitro* assays was 1%. The compounds were tested in an AlamarBlue serial drug dilution assay[16] to determine the 50% inhibitory concentrations (IC_{50}). Serial drug dilutions were prepared in 96-well microtiter plates containing the culture medium, and wells were inoculated with 2.0 × 10^4 cells/mL *T. b. rhodesiense* IL-1501 parasites. Cultures were incubated for 69 h at 37 °C under a humidified 5% CO_2 atmosphere. After this time, 10 μL of resazurin (12.5 mg of resazurin [Sigma] dissolved in 100 mL of phosphate-buffered saline) was added to each well. The plates were incubated for an additional 3 h. The plates were read in a SpectraMax Gemini XS microplate fluorescence scanner (Molecular Devices) using an excitation wavelength of 536 nm and an emission wavelength of 588 nm.

Conformational Search for the Two Model Compounds of the Prenyl Tryptophan Moiety, (8*S*,10*S*,16*S*)-2 and (8*S*,10*R*,16*R*)-2. The conformational search for the two model compounds (8*S*,10*S*,16*S*)-**2** and (8*S*,10*R*,16*R*)-**2** was carried out using the MMFF force field and torsional sampling of the Macro Model program.[17] An energy window cutoff of 10.0 kcal/mol was used during the conformational search. Redundant conformers were eliminated using an RMSD cutoff of 1.0 Å. Then, all conformers were subjected to geometry optimization using the Gaussian 16 package[18] in the gas phase at the B3LYP/6-31G* level. The resulting conformers were further optimized at the B3LYP level of theory using the def2-SVP basis set with PCM[19] in MeCN using the Gaussian 16 package.[18] As a result, we obtained seven conformers for (8*S*,10*S*,16*S*)-**2** and 15 conformers for (8*S*,10*R*,16*R*)-**2** as the conformers that have a calculated Boltzmann weight of more than 1%.

ECD Calculation Methods. The optimized conformers of (8*S*,10*S*,16*S*)-**2** and (8*S*,10*R*,16*R*)-**2** that showed >1% Boltzmann population were used for ECD calculations using TDDFT[20] with PCM[19] in MeCN. We used the four different combinations of functional and basis set as follows: B3LYP/def2-SVP, ωB97X-D/def2-SVP, cam-B3LYP/def2-SVP, and ωB97X-D/6-311+G*, respectively. ECD curves were generated with Spec Dis software using a half-bandwidth of 0.16 eV.[21] The relative populations of each conformer were calculated based on the Boltzmann weighting factor at 298.15 K. UV correction of +20 nm for B3LYP/def2-SVP, +35 nm for ωB97X-D/def2-SVP and cam-B3LYP/def2-SVP, and +25 nm for ωB97X-D/6-311+G* were applied for proper comparison. All calculated spectra were scaled by a factor of 1/2 to enable comparison with the experimental spectrum.

■ ASSOCIATED CONTENT

Supporting Information

The Supporting Information is available free of charge at https://pubs.acs.org/doi/10.1021/acs.jnatprod.1c00234.

NMR spectra for motobamide (**1**); HPLC chromatograms for determination of the absolute configurations; phylogenetic tree of the cyanobacterial sample, detailed results of the computational chemistry (PDF)

■ AUTHOR INFORMATION

Corresponding Author

Kiyotake Suenaga − *Department of Chemistry, Faculty of Science and Technology, Keio University, Yokohama, Kanagawa 223-8522, Japan*; Email: suenaga@chem.keio.ac.jp

Authors

Hiroki Takahashi − *Department of Chemistry, Faculty of Science and Technology, Keio University, Yokohama, Kanagawa 223-8522, Japan*

Arihiro Iwasaki − *Department of Chemistry, Faculty of Science and Technology, Keio University, Yokohama, Kanagawa 223-8522, Japan*; orcid.org/0000-0002-3775-5066

Naoaki Kurisawa − *Department of Chemistry, Faculty of Science and Technology, Keio University, Yokohama, Kanagawa 223-8522, Japan*

Ryota Suzuki − *S&E Simulation, Yokohama, Kanagawa 234-0052, Japan*

Ghulam Jeelani − *Department of Biomedical Chemistry, Graduate School of Medicine, The University of Tokyo, Tokyo 113-0033, Japan*

Teruhiko Matsubara − *Department of Biosciences and Informatics, Faculty of Science and Technology, Keio*

University, Yokohama, Kanagawa 223-8522, Japan; orcid.org/0000-0002-8006-4324

Toshinori Sato − *Department of Biosciences and Informatics, Faculty of Science and Technology, Keio University, Yokohama, Kanagawa 223-8522, Japan;* orcid.org/0000-0002-4429-6101

Tomoyoshi Nozaki − *Department of Biomedical Chemistry, Graduate School of Medicine, The University of Tokyo, Tokyo 113-0033, Japan*

Complete contact information is available at: https://pubs.acs.org/10.1021/acs.jnatprod.1c00234

Notes

The authors declare no competing financial interest.

■ ACKNOWLEDGMENTS

This work was supported by JSPS KAKENHI (Grant Numbers 18K14346 and 20H02870).

■ REFERENCES

(1) Büscher, P.; Cecchi, G.; Jamonneau, V.; Priotto, G. *Lancet* **2017**, *390*, 2397−2409.
(2) Sanchez, L. M.; Knudsen, G. M.; Helbig, C.; Muylder, G. D.; Mascuch, S. M.; Mackey, Z. B.; Gerwick, L.; Clayton, C.; McKerrow, J. H.; Linington, R. G. *J. Nat. Prod.* **2013**, *76*, 630−641.
(3) Iwasaki, K.; Iwasaki, A.; Sumimoto, S.; Matsubara, T.; Sato, T.; Nozaki, T.; Saito-Nakano, Y.; Suenaga, K. *J. Nat. Prod.* **2020**, *83*, 481−488.
(4) Schubert, M.; Labudde, D.; Oschkinat, H.; Schmieder, P. *J. Biomol. NMR* **2002**, *24*, 149−154.
(5) Ishida, K.; Matsuda, H.; Murakami, M.; Yamaguchi, K. *Tetrahedron* **1996**, *52*, 9025−9030.
(6) Phyo, M. Y.; Ding, C. Y. G.; Goh, H. C.; Goh, J. X.; Ong, J. F. M.; Chan, S. H.; Yung, P. Y. M.; Candra, H.; Tan, L. T. *J. Nat. Prod.* **2019**, *82*, 3482−3488.
(7) Engene, N.; Tronholm, A.; Paul, V. J. *J. Phycol.* **2018**, *54*, 435−446.
(8) Pruesse, E.; Peplies, J.; Glöckner, F. O. *Bioinformatics* **2012**, *28*, 1823−1829.
(9) (a) Talavera, G.; Castresana, J. *Syst. Biol.* **2007**, *56*, 564−577. (b) Castresana, J. *Mol. Biol. Evol.* **2000**, *17*, 540−552.
(10) Darriba, D.; Taboada, G. L.; Doallo, R.; Posada, D. *Nat. Methods* **2012**, *9*, 772.
(11) Guindon, S.; Gascuel, O. *Syst. Biol.* **2003**, *52*, 696−704.
(12) Perrière, G.; Gouy, M. *Biochimie* **1996**, *78*, 364−369.
(13) Ronquist, F.; Teslenko, M.; van der Mark, P.; Ayres, D. L.; Darling, A.; Höhna, S.; Larget, B.; Liu, L.; Suchard, M. A.; Huelsenbeck, J. P. *Syst. Biol.* **2012**, *61*, 539−542.
(14) Kuboki, N.; Inoue, N.; Sakurai, T.; Cello, F. D.; Grab, D. J.; Susuki, H.; Sugimoto, C.; Igarashi, I. *J. Clin. Microbiol.* **2003**, *41*, 5517−5524.
(15) Räz, B.; Iten, M.; Grether-Bühler, Y.; Kaminsky, R.; Brun, R. *Acta Trop.* **1997**, *68*, 139−147.
(16) Huber, W.; Koella, J. C. *Acta Trop.* **1993**, *55*, 257−261.
(17) *Schrödinger Release 2021-1: Macromodel*; Schrödinger, LLC: New York, NY, 2021.
(18) Frisch, M. J.; Trucks, G. W.; Schlegel, H. B.; Scuseria, G. E.; Robb, M. A.; Cheeseman, J. R.; Scalmani, G.; Barone, V.; Petersson, G. A.; Nakatsuji, H.; Li, X.; Caricato, M.; Marenich, A. V.; Bloino, J.; Janesko, B. G.; Gomperts, R.; Mennucci, B.; Hratchian, H. P.; Ortiz, J. V.; Izmaylov, A. F.; Sonnenberg, J. L.; Williams-Young, D.; Ding, F.; Lipparini, F.; Egidi, F.; Goings, J.; Peng, B.; Petrone, A.; Henderson, T.; Ranasinghe, D.; Zakrzewski, V. G.; Gao, J.; Rega, N.; Zheng, G.; Liang, W.; Hada, M.; Ehara, M.; Toyota, K.; Fukuda, R.; Hasegawa, J.; Ishida, M.; Nakajima, T.; Honda, Y.; Kitao, O.; Nakai, H.; Vreven, T.; Throssell, K.; Montgomery, J. A., Jr.; Peralta, J. E.; Ogliaro, F.; Bearpark, M. J.; Heyd, J. J.; Brothers, E. N.; Kudin, K. N.; Staroverov, V. N.; Keith, T. A.; Kobayashi, R.; Normand, J.; Raghavachari, K.; Rendell, A. P.; Burant, J. C.; Iyengar, S. S.; Tomasi, J.; Cossi, M.; Millam, J. M.; Klene, M.; Adamo, C.; Cammi, R.; Ochterski, J. W.; Martin, R. L.; Morokuma, K.; Farkas, O.; Foresman, J. B.; Fox, D. J. *Gaussian 16*, Revision C.01; Gaussian, Inc.: Wallingford, CT, 2016.
(19) Tomasi, J.; Mennucci, B.; Cammi, R. *Chem. Rev.* **2005**, *105*, 2999−3094.
(20) Autschbach, J. *ChemPhysChem* **2011**, *12*, 3224−3235.
(21) Bruhn, T.; Schaumlöffel, A.; Hemberger, Y.; Bringmann, G. *Chirality* **2013**, *25*, 243−249.